# Supporting Information

# Enhancing anticancer efficacy of nitric oxide and formaldehyde co-donor through isotope substitution

Ziyao Zhao [a,1], Yu Zhang [a,1]*, Chunyuan Hou [a], Jun Wan [a], Peicheng Wang [a], Xijie Feng [b], Jun Luo [a,*]

[a] *School of Chemistry and Chemical Engineering, Nanjing University of Science and Technology, Nanjing 210094, China.*
[b] *School of Pharmaceutics, China Pharmaceutical University, Nanjing 210009, China.*

* To whom correspondence should be addressed. E-mail: y_zhang@njust.edu.cn (Y. Zhang), luojun@njust.edu.cn (J. Luo).
[1] These authors contributed equally to this work.

# 1. Experimental section and supporting figures

**Materials and instrument**

$NH_4{}^{15}NO_3$ is provided by Shanghai Research Institute of Chemical Industry CO., 7LTD. Paraformaldehyde-$d_2$ was purchased from Adamas. Other chemicals (AR grade) were obtained from commercial sources and used without further purification. Methyl thiazolyl tetrazolium (MTT), Hoechst 3342 and 2'-7'dichlorofluorescin diacetate (DCFH-DA) were bought from Beyotime Institute of Biotechnology Co. LLC. (Nantong). Calcein/PI Cell Viability/Cytotoxicity Assay Kit and JC-1 Assay Kit were purchased from KeyGEN Bio TECH Corp., Ltd (Nanjing).

$^1$H-NMR and $^{13}$C-NMR spectra were recorded on a AVANCE NEO 500MHz using DMSO-$d_6$ and $CDCl_3$ as solvent. IR spectra were recorded with a Thermo NICOLETIS20. MTT assays were performed on a microplate reader (Tecan Group). DLS was performed on Zetasizer (Nano ZS, Malvern U.K.). TEM images were taken with an H-800 transmission electron microscope (Hitachi). Fluorescent images were taken by an inverted fluorescence microscope (Nikon Instruments). *In vivo* images were obtained on PerkinElmer IVIS Spectrum (PerkinElmer).

**Cell line and animals**

The B16F10 cell line was obtained from Cell Bank of Chinese Academy of Sciences. B16F10 cell line was cultured in RPMI 1640 medium supplemented with 10% FBS (Gibco) and penicillin/streptomycin (1%, w/v), respectively. B16F10 cell line was cultured in incubator at 37℃ under an atmosphere of 5% $CO_2$ and 90% relative humidity. C57BL/6 mice and Sprague Dawley rats were purchased from Jiangsu Huachuang Biotechnology Co., LTD. C57BL/6 mice used in experiments were 6-8 weeks old and SD rats used in experiments were 3-4 weeks. All animal experiments were performed in accordance with the National Institute of Health Guidelines under the protocols approved by the Animal Ethical and Welfare Committee of Nanjing University of Science and Technology (Approval No: AUCU-NUST2023012).

**Synthesis**

*Synthetic procedures and identification of 3,7-dinitro-1,3,5,7-tetraazabicyclo[3.3.1] nonane. (DPT)*

To a stirred acetic acid (0.60 mL, 10.00 mmol) were continuously and equivalently added a solution of urotropine (HA) (1.40 g, 10.00 mmol) in acetic acid (2.30 mL, 40.00 mmol) and a solution of fuming nitric acid (0.90 mL, 21.00 mmol) in acetic anhydride (2.80 mL, 30.00 mmol) at 25 °C for 60 min. After that, the reaction mixture was stirred another 30 min at the same temperature. The reaction was then quenched by the addition of hot water (20 mL, 65 °C). The precipitated product was filtered, washed with pure water, and dried to afford DPT as white powder in 79.20% yield.$^1$H-NMR (DMSO-$d_6$, 500 MHz) δ = 5.50 (d, 4 H, J = 13.0 Hz), 4.94 (d, 4 H, J = 13.0 Hz), 4.12 (s, 2 H) ppm; $^{13}$C-NMR (DMSO-$d_6$, 126 MHz) δ = 69.17, 65.57 ppm. IR (υ/cm$^{-1}$): 3053, 3000, 2933, 2877, 1627, 1521, 1489, 1272, 1190, 1078, 921, 824, 766 and 643 cm$^{-1}$. ESI-MS: m/z [(M+H)$^+$]: 219.21.

*Synthetic procedures and identification of deuterated urotropine (HA-$d_{12}$)*

The deuterated paraformaldehyde (paraformaldehyde-$d_2$) (1.10 g, 31.60 mmol) was charged into a three-necked flask. $H_2O$ (2 mL) was added, followed by the dropwise addition of aqueous ammonia (3 mL, 25-28%) at room temperature. The mixture was heated to 40 °C in an oil bath under reflux for 24 h. Distillation under reduced pressure yielded 0.76 g of a white solid (HA-$d_{12}$), representing a 94.20% yield.$^{13}$C NMR (126 MHz, $CDCl_3$) δ = 74.21, 74.03, 73.85, 73.67, 73.49 ppm.

*Synthetic procedures and identification of deuterated 3,7-dinitro-1,3,5,7-tetraazabicyclo[3.3.1] nonane-$d_{10}$ (DPT-$d_{10}$).*

To a stirred acetic acid (0.60 mL, 10.00 mmol) were continuously and equivalently added a solution of HA-$d_{12}$ (1.40 g, 10.00 mmol) in acetic acid (2.30 mL, 40.00 mmol) and a solution of fuming nitric acid (0.90 mL, 21.00 mmol) in acetic anhydride (2.80 mL, 30.00 mmol) at 25 °C for 60 min. After that, the reaction mixture was stirred another 30 min at the same temperature. The reaction was then quenched by the addition of hot water (20 mL,65 °C). The precipitated product was filtered, washed with pure water, and dried to obtain DPT-$d_{10}$ as white powder in 60.20 % yield.$^{13}$C-NMR (DMSO-$d_6$, 126 MHz) δ = 68.75, 68.56, 68.36, 68.17, 67.98, 64.54 ppm. IR (υ/cm$^{-1}$): 2253, 2169, 2144, 2124, 1625, 1515, 1489, 1224, 1183, 1049, 867, 761, 726, 610 cm$^{-1}$. ESI-MS: m/z [(M+H)$^+$]: 229.15.

*Synthetic procedures and identification of nitro-$^{15}$N-substituted 3,7-dinitro-1,3,5,7-tetraazabicyclo[3.3.1] nonane-$^{15}NO_2$ (DPT-$^{15}N_2$).*

A solution of HA in acetic acid was prepared by adding 1.40 g (10.00 mmol) of HA and 2.30 mL (40.00 mmol) of acetic acid to a 25 mL round-bottom flask, followed by stirring at room temperature until complete dissolution. Separately, an acetic anhydride-methanesulfonic acid mixture was prepared in an ice bath by adding 2.80 mL (30.00 mmol) of acetic anhydride to another 25 mL round-bottom flask, then slowly dripping in 1.30 mL (20.00 mmol) of methanesulfonic acid with thorough mixing. In a 50 mL round-bottom flask, 0.60 mL (10.00 mmol) of acetic acid and 2.00 g (25.00 mmol) of $NH_4{}^{15}NO_3$ were combined and stirred in an oil bath at 25 °C for 15 min. With continuous stirring, both the HA-acetic acid solution and the mixed anhydride-acid solution were added simultaneously *via* constant-pressure dropping funnels over 1 h. After completion of addition, the reaction mixture was maintained at 25 °C for 0.50 h. The reaction was quenched with 20 mL of warm water (65 °C), and the resulting white solid was filtered and vacuum-dried to afford 0.65 g of DPT-$^{15}N_2$, giving a 38.00% yield. $^1$H-NMR (DMSO-$d_6$, 500 MHz) δ = 5.51 (d, 4 H, J = 13.0 Hz), 4.95 (d, 4 H, J = 13.0 Hz), 4.13 (s, 2 H) ppm; $^{13}$C-NMR (DMSO-$d_6$, 126 MHz) δ = 69.09, 65.41 ppm. IR (υ/cm$^{-1}$): 3053, 3000, 2933, 2877, 1592,1490, 1452, 1242, 1189, 1078, 921, 824, 775, 643 cm$^{-1}$.m/z [(M+H)$^+$]: 221.07.

*Synthetic procedures and identification of dual-modified 3,7-dinitro-1,3,5,7-tetraazabicyclo[3.3.1] nonane-$d_{10}$ (DPT-$^{15}N_2$+$d_{10}$).*

A solution of HA-$d_2$ in acetic acid was prepared by adding 1.40 g (10.00 mmol) of HA-$d_2$ and 2.30 mL (40.00 mmol) of acetic acid to a 25 mL round-bottom flask, followed by stirring at room temperature until complete dissolution. Separately, an acetic anhydride-methanesulfonic acid mixture was prepared in an ice bath by adding 2.80 mL (30.0 mmol) of acetic anhydride to another 25 mL round-bottom flask, then slowly dripping in 1.30 mL (20.00 mmol) of methanesulfonic acid with thorough mixing. In a 50 mL round-bottom flask, 0.60 mL (10.00 mmol) of acetic acid and 2.00 g (25.00 mmol) of $NH_4{}^{15}NO_3$ were combined and stirred in an oil bath at 25 °C for 15 min. With continuous stirring, both the HA-$d_2$-acetic acid solution and the mixed anhydride-acid solution were added simultaneously *via* constant-pressure dropping funnels over 1 h. After completion of addition, the reaction mixture was maintained at 25 °C for 0.50 h. The reaction was quenched with 20 mL of warm water (65 °C), and the resulting white solid was filtered and vacuum-dried to afford 0.59 g of DPT-$^{15}N_2$+$d_{10}$, giving a 35.00% yield. $^{13}$C-NMR (DMSO-$d_6$, 126 MHz) δ = 68.57, 68.57, 68.19, 64.56. IR (υ/cm$^{-1}$): 2253, 2169, 2144, 2124, 1584, 1479, 1455, 1219, 1184, 1049, 865, 747, 726, 608 cm$^{-1}$. ESI-MS: m/z [(M+H)$^+$]: 231.14.

**Preparation and characterization of lipo@DPT, lipo@DPT-$d_{10}$, lipo@DPT-$^{15}N_2$, and lipo@DPT-$^{15}N_2$+$d_{10}$.**

lipo@DPT, lipo@DPT-$d_{10}$, lipo@DPT-$^{15}N_2$, and lipo@DPT-$^{15}N_2$+$d_{10}$ were prepared using the thin lipid film hydration and sequential extrusion method. HSPC, cholesterol, DSPE-mPEG2000, and DPT, DPT-$d_{10}$, DPT-$^{15}N_2$ or DPT-$^{15}N_2$+$d_{10}$ (5:3:1.5:1, w/w) were dissolved in a mixture of chloroform and methanol (1:2, v/v). The solution was evaporated by rotary evaporation to form a homogeneous film. The film was hydrated with 1 mL deionized water at 60 °C and sonicated for 5 min in an ice bath. Subsequently, the liposome suspension was extruded sequentially 21 times through polycarbonate membrane filters with pore sizes of 800, 400 and 200 nm, respectively. Products were purified by a Sephadex G50 column.

**Assessment of EE and DL**

lipo@DPT, lipo@DPT-$d_{10}$, lipo@DPT-$^{15}N_2$, and lipo@DPT-$^{15}N_2$+$d_{10}$ were separately broken by adding the mixture of chloroform and methanol (1:2, v/v), and the amounts of compound were measured using the highperformance liquid chromatography (HPLC) method (Shimadzu LC-20A) with reverse phase S7 micro C18 column. The eluent used was a mixture of acetonitrile, methanol and water (5 : 35 : 60) with a flow rate 1 mL/min, and the detection was conducted at a wavelength of 224 nm. The DL and EE were calculated as follows:

$$DL\ (\%) = M_d/M_s \times 100\%$$

$$EE\ (\%) = M_d/M_o \times 100\%$$

where $M_d$ represents the total amount of drug in liposome, $M_s$ represents the total amount of drug and liposomal formula, and $M_o$ represents the initial amount of drug used to prepare liposome.

***In vitro* cytotoxicity**

For MTT assay, cancer cells B16F10 were seeded in 96-well plates in complete medium overnight, followed by incubating with different concentrations of DPT, DPT-$d_{10}$, DPT-$^{15}N_2$, DPT-$^{15}N_2$+$d_{10}$ lipo@DPT, lipo@DPT-$d_{10}$, lipo@DPT-$^{15}N_2$, or lipo@DPT-$^{15}N_2$+$d_{10}$ for 24 h. MTT solution (20 μL) was added to the culture medium, and the medium was removed after 4 h of incubation, followed by adding dimethyl sulfoxide (200 μL). The absorbance of individual well was measured at 570 nm using the microplate reader.

**NO release evaluation**

Total NO production was estimated by measurement of the accumulation of nitrite and nitrate using the Griess reagent in the Total Nitric Oxide Assay Kit (Beyotime, China). The B16F10 cells ($5 \times 10^3$ cells per well) were seeded in 96-well plates in complete medium overnight, followed by incubating with 0.8 mM of DPT, DPT-$d_{10}$, DPT-$^{15}N_2$, or DPT-$^{15}N_2$+$d_{10}$, and 0.95 mM of lipo@DPT, lipo@DPT-$d_{10}$, lipo@DPT-$^{15}N_2$ or lipo@DPT-$^{15}N_2$+$d_{10}$ for 2 h or 12 h. Nitrate was measured after enzymatic conversion to nitrite by nitrate reductase.Briefly, the lysis buffer of every sample was added in duplicate wells in a 96-well plate at room temperature. The mixture was incubated with 5 μL of nicotinamide adenine dinucleotide phosphate (NADPH), 10 μL of flavin adenine dinucleotide (FAD) and 5 μL of nitrate reductase for 30 min at 37°C. Then, 10 μL of lactate dehydrogenase (LDH) buffer and 10 μL of LDH were added to the above mixture for another 30 min at 37°C. Finally, 50 μL of Griess reagent I and 50 μL of Griess reagent II were added into the wells before incubation for 10 min. The absorbance of individual well was measured at 540 nm using the microplate reader. Concentrations were calculated using a standard curve (80, 60, 40, 20, 10, 5 and 2 μM sodium nitrite).

**Formaldehyde release evaluation**

Formaldehyde Assay Kit (Sigma-Aldrich, the USA) was used to evaluate the formaldehyde release. The B16F10 cells ($5 \times 10^3$ cells per well) were seeded in 96-well plates in complete medium overnight, followed by incubating with 0.80 mM of DPT, DPT-$d_{10}$, DPT-$^{15}N_2$, or DPT-$^{15}N_2$+$d_{10}$, and 0.95 mM of lipo@DPT, lipo@DPT-$d_{10}$, lipo@DPT-$^{15}N_2$ or lipo@DPT-$^{15}N_2$+$d_{10}$ for 2 h or 12 h. Formaldehyde was measured after deproteinated and neutralized the protein in samples. Add 50μL of 10% TCA per 100 μL of sample. Vortex and centrifuge for 5 min at 14,000 rpm. Transfer 100 μL of clear supernatant to a clean plate and neutralize with 25 μL of Neutralizer. Briefly, 50 μL of Reaction Mix was transferred to each of the samples and tapped plate briefly to mix. Incubate the samples at room temperature for 30 min protected from light. The fluorescence intensity of individual well was measured at $E_x/E_m$ = 370/470 nm. Concentrations were calculated using a standard curve (0, 30, 60 and 100 μM of formaldehyde).

**Measurement of intracellular ROS levels**

B16F10 cells in 24-well plates ($1 \times 10^5$ cells per well) were grown overnight to reach 70-90% confluence, followed by incubating with 0.8 mM of DDPT, DPT-$d_{10}$, DPT-$^{15}N_2$, or DPT-$^{15}N_2$+$d_{10}$, and 0.95 mM of lipo@DPT, lipo@DPT-$d_{10}$, lipo@DPT-$^{15}N_2$ or lipo@DPT-$^{15}N_2$+$d_{10}$ for 2 h or 12 h. After washing three times with PBS, the cells were incubated with DCFH-DA (1 μL, 10 mM) and Hoechst 33342 (1 μL, 1 mM) for 30 min in fresh culture medium (0.50 mL), and imaged by inverted fluorescence microscope ($E_x/E_m$ = 495/529 nm for DCFH-DA and $E_x/E_m$ = 350/460 nm for Hoechst 33342) and analyzed using ImageJ programs.

**Measurement of mitochondrial membrane potential**

The mitochondrial membrane potential changes were measured using a JC-1 Assay Kit. B16F10 cells were seeded into confocal dishes ($5 \times 10^5$ cells per dish) and cultured at 37 °C for 24 h, followed by incubating with saline, CCCP (0.01 mM), DPT (0.80 mM), DPT-$d_{10}$ (0.80 mM), DPT-$^{15}N_2$ (0.8 mM), DPT-$^{15}N_2$+$d_{10}$ (0.80 mM), lipo@DPT (0.95 mM), lipo@DPT-$d_{10}$ (0.95 mM), lipo@DPT-$^{15}N_2$ (0.95 mM), or lipo@DPT-$^{15}N_2$+$d_{10}$ (0.95 mM) for 12 h. Depolarization of the mitochondrial membrane is characterized by a shift from red fluorescence to green fluorescence. The simultaneous measurement of fluorescence was performed by inverted fluorescence microscope. The green fluorescent emission ($E_x/E_m$ = 514/529 nm) of J-monomerand and red fluorescent emission ($E_x/E_m$ = 585/590 nm) of Jaggregate were measured and analyzed using ImageJ programs.

**Cellular uptake**

B16F10 cells were seeded in 12-well plates ($2.5 \times 10^5$ cells per well). The 12-well plates were placed in an incubator at 37°C with an atmosphere of 5% $CO_2$ and 90% relative humidity, and grown overnight until they reached around 70-90% confluence. Then, the cells were incubated with FITC-labeled lipo@DPT, lipo@DPT-$d_{10}$,

lipo@DPT-$^{15}N_2$, or lipo@DPT-$^{15}N_2$+$d_{10}$. Cells were harvested at different time points (1, 2, 4, 8, 12 and 24 h), and stained with Hoechst 33342 (1 μL, 1 mM) for 15 min, washed three times with PBS, and then imaged with fluorescence microscope ($E_x/E_m$ = 488/525 nm for FITC, $E_x/E_m$ =350/460 nm for Hoechst 33342). The fluorescence intensity was quantified by ImageJ programs.

***In vivo* tumor targeting and biodistribution**

For *in vivo* experiments, B16F10 cells ($1 \times 10^7$) were subcutaneously injected into female C57BL/6 mice. When tumor volume reached ≈ 100 $mm^3$, mice were randomly assigned to five different groups (n = 5), and were used to evaluate the tumor targeting and biodistribution of lipo@DPT, lipo@DPT-$d_{10}$, lipo@DPT-$^{15}N_2$, and lipo@DPT-$^{15}N_2$+$d_{10}$. DiR-labeled lipo@DPT (2.50 mg·$kg^{-1}$ of DPT, 1.00 mg·$kg^{-1}$ of DiR) , lipo@DPT-$d_{10}$ (2.50 mg·$kg^{-1}$ of DPT-$d_{10}$, 1.00 mg·$kg^{-1}$ of DiR), lipo@DPT-$^{15}N_2$(2.50 mg·$kg^{-1}$ of DPT-$^{15}N_2$, 1.00 mg·$kg^{-1}$ of DiR) or lipo@DPT-$^{15}N_2$+$d_{10}$ (2.50 mg·$kg^{-1}$ of DPT-$^{15}N_2$+$d_{10}$, 1.00 mg·$kg^{-1}$ of DiR) was injected into mice via the tail vein. The tumor region was imaged at the indicated time (4, 8, 12, and 24 h). Moreover, after 24 h injection of DiR-labeled liposome, the tumor-bearing mice were sacrificed, and major organs were obtained and imaged**.**

**Pharmacokinetic studies in rats**

Sprague Dawley rats were used to evaluate the pharmacokinetics of DPT, DPT-$d_{10}$, DPT-$^{15}N_2$ and DPT-$^{15}N_2$+$d_{10}$. The concentrations of DPT, DPT-$d_{10}$, DPT-$^{15}N_2$ and DPT-$^{15}N_2$+$d_{10}$ in plasma were measured using HPLC. DPT (2.50 mg·$kg^{-1}$), DPT-$d_{10}$ (2.50 mg·$kg^{-1}$), DPT-$^{15}N_2$ (2.50 mg·$kg^{-1}$) or DPT-$^{15}$NO+$d_{10}$ (2.50 mg·$kg^{-1}$) were separately injected through the tail vein (n = 5), and blood samples were collected at predetermined intervals. Plasma was obtained by centrifugation at 10 000 rpm for 10 min, followed by adding 200 μL of acetonitrile. The mixture was vortexed for 2 min, centrifuged at 12 000 rpm for 10 min, and measured by HPLC. Pharmacokinetic parameters were calculated by PKSolver V2.0.

***In vivo* antitumor effects**

Female C57BL/6 mice bearing B16F10 tumors were intravenously injected with saline (control), lipo@DPT (2.50 mg·$kg^{-1}$ of DPT), lipo@DPT-$d_{10}$ (2.50 mg·$kg^{-1}$ of DPT-$d_{10}$), lipo@DPT-$^{15}N_2$ (2.50 mg·$kg^{-1}$ of DPT-$^{15}N_2$) or lipo@DPT-$^{15}N_2$+$d_{10}$ (2.50 mg·$kg^{-1}$ of DPT-$^{15}N_2$+$d_{10}$) every 2 days for 10 days. Tumor volumes and body weights were measured every 2 days. At the end of the experiments, mice were sacrificed, and tumors were collected, weighted, imaged, and analyzed by H&E, Tunel and ROS. The major organs, including heart, liver, spleen, lung, and kidneys were also harvested and analyzed by H&E stains.

**Assessment of Synergistic Effect between Deuteration and Nitro-$^{15}$N Substitution**

To quantitatively evaluate whether deuterium (D) and nitro-$^{15}$N substitution exert a synergistic anticancer effect, the Bliss independence model was employed. This model discriminates the nature of drug interactions by comparing the experimentally observed combined effect with the expected effect calculated under the assumption of independent action. An observed value exceeding the expected value indicates synergy, a lower value suggests antagonism, and comparable values imply an additive effect.In this study, the liposomal formulation containing only nitro-$^{15}$N substitution (lipo@DPT-$^{15}N_2$) and that containing only deuteration (lipo@DPT-$d_{10}$) were treated as two independent interventions. Their respective single-agent tumor volume inhibition rates were taken as the effect fractions, denoted as $E_a$ (0.64) and $E_e$ (0.61). The expected combined effect was calculated according to the Bliss model:

$$E_{expected} = E_a + E_e - (E_a \times E_e)$$

$$= 0.64 + 0.61 - (0.64 \times 0.61)$$

$$= 0.86$$

The experimentally measured tumor inhibition rate for the dual-modified formulation (lipo@DPT-$^{15}$N+$d_{10}$), Eobserved, was 0.88. Since the observed value (0.88) is greater than the theoretically expected value (0.86), the results demonstrate that deuteration and nitro-$^{5}$N substitution exhibit a clear synergistic effect in enhancing the antitumor activity of DPT.

**Statistics**

All experiments were repeated at least three times. Data are represented as mean ± SD. Error bars represent standard error of the mean from independent samples assayed within the experiments. Statistical analysis was done with GraphPad Prism 6 software. Statistical significance was calculated using two-tailed Student's *t*-test: * represents $P < 0.05$, ** represent $P < 0.01$, and *** represent $P < 0.001$.

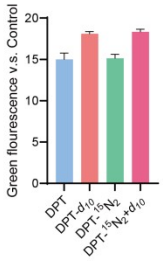


Figure S1 Fluorescence intensity of ROS in B16F10 cells after treatment with 0.80 mM DPT, DPT-$d_{10}$, DPT-$^{15}N_2$ and DPT-$^{15}N_2$+$d_{10}$. The data are presented as mean ± SD (n = 6).

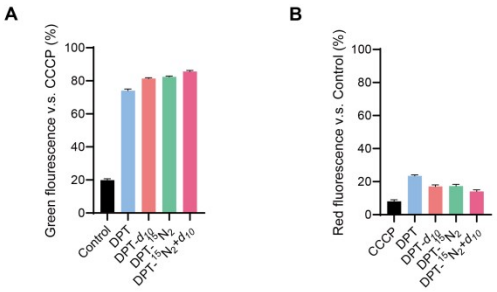


Figure S2 Mitochondrial membrane potentials in B16F10 cells were determined by JC-1 assay after 12 h of incubation with 0.8 mM DPT, DPT-$d_{10}$, DPT-$^{15}N_2$ and DPT-$^{15}N_2$+$d_{10}$. The data are presented as mean ± SD (n = 6).

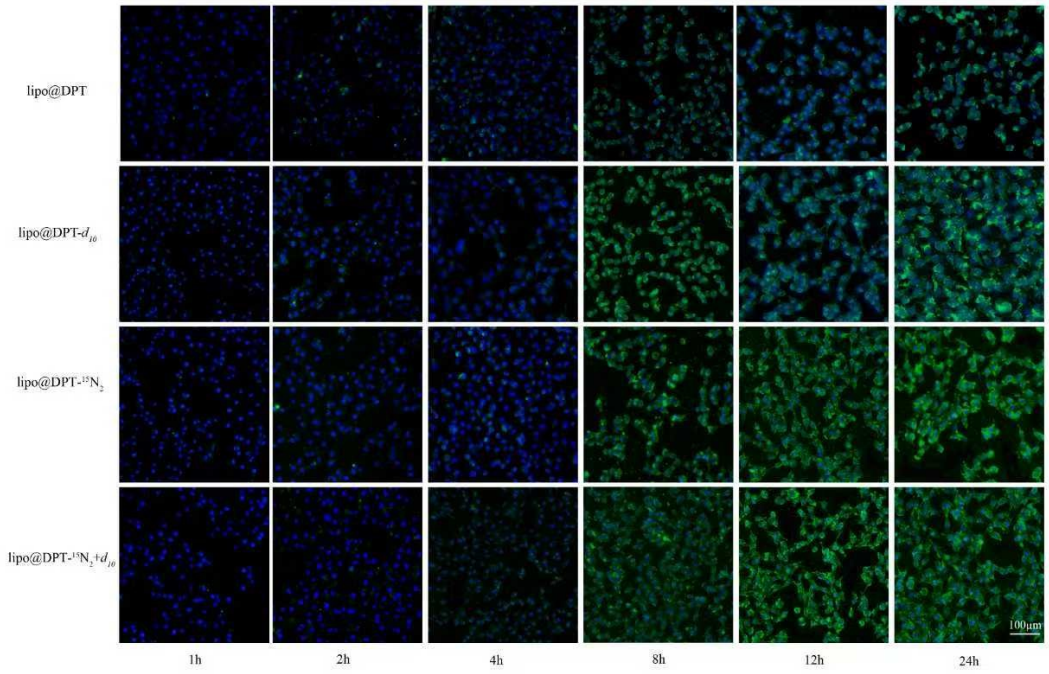


Figure S3 Cellular uptake fluorescent images of FITC-labeled lipo@DPT, lipo@DPT-$d_{10}$, lipo@DPT-$^{15}N_2$, and lipo@DPT-$^{15}N_2$+$d_{10}$. The data are presented as mean ± SD (n = 6).

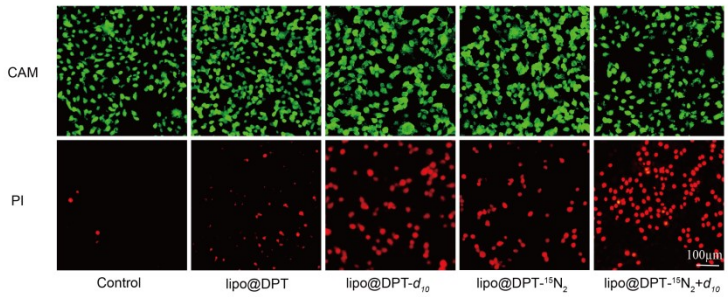


Figure S4 Fluorescence images of calcein AM (green) and propidium iodide (PI, red) B16F10 cells after t reatment with 0.95 mM lipo@DPT, lipo@DPT-$d_{10}$, lipo@DPT-$^{15}N_2$, and lipo@DPT-$^{15}N_2$+$d_{10}$. The data are p resented as mean ± SD (n = 6).

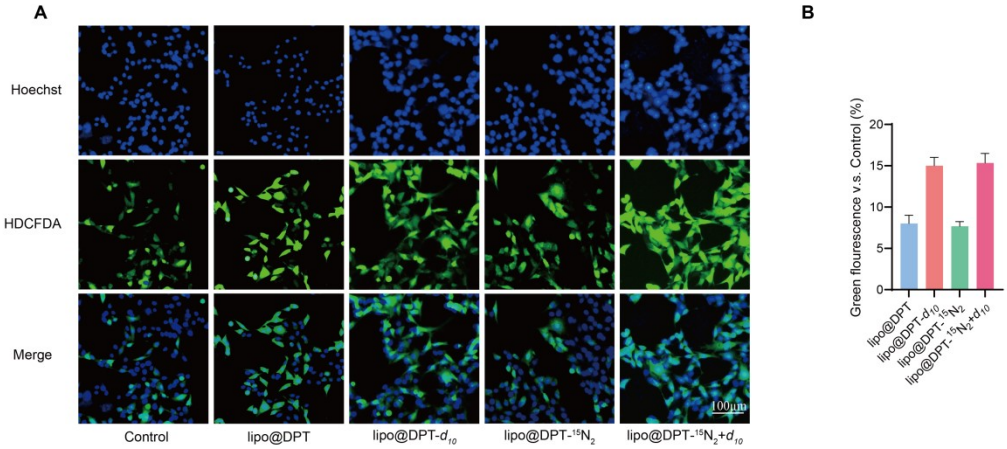


Figure S5 Fluorescence images and fluorescence intensity of intracellular ROS in B16F10 cells stained wi th DCFH-DA, treated with 0.95 mM of lipo@DPT, lipo@DPT-$d_{10}$, lipo@DPT-$^{15}N_2$, and lipo@DPT-$^{15}N_2$+$d_{10}$. The data are presented as mean ± SD (n = 6).

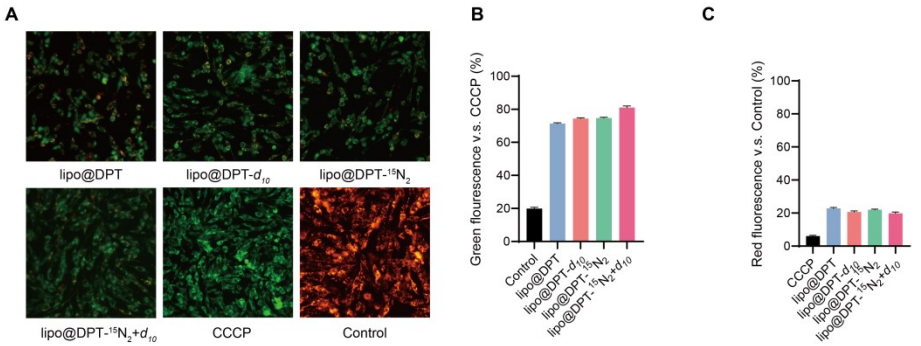


Figure S6 Mitochondrial membrane potentials of B16F10 cells after 24 h of incubation with 0.95 mM lipo@DPT, lipo@DPT-$d_{10}$, lipo@DPT-$^{15}N_2$, and lipo@DPT-$^{15}N_2$+$d_{10}$. The data are presented as mean ± SD (n = 6).

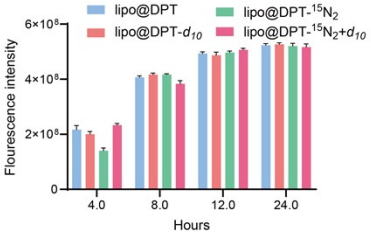


Figure S7 Time-dependent fluorescent intensity of the tumors. Tumor bearing mice were intravenously i

njected with lipo@DPT (2.50 mg·kg$^{-1}$ of DPT, 1.0 mg·kg$^{-1}$ of DiR) , lipo@DPT-$d_{10}$ (2.50 mg·kg$^{-1}$ of DPT-$d_{10}$, 1.00 mg·kg$^{-1}$ of DiR) , lipo@DPT-$^{15}N_2$ (2.50 mg·kg$^{-1}$ of DPT-$^{15}N_2$, 1.00 mg·kg$^{-1}$ of DiR) or lipo@DPT-$^{15}N_2$+$d_{10}$ (2.50 mg·kg$^{-1}$ of DPT-$^{15}N_2$+$d_{10}$, 1.00 mg·kg$^{-1}$ of DiR), and the fluorescent intensity of tumor areas w as monitored for 24 h. The data are presented as mean ± SD (n = 5).

Figure S8 Quantification of fluorescence intensity of major organs and tumors after intravenous injection of DiR-labelled lipo@DPT (2.50 mg·kg$^{-1}$ of DPT, 1.00 mg·kg$^{-1}$ of DiR) , lipo@DPT-$d_{10}$ (2.5 mg·kg$^{-1}$ of DPT-$d_{10}$, 1.00 mg·kg$^{-1}$ of DiR) , lipo@DPT-$^{15}N_2$ (2.50 mg·kg$^{-1}$ of DPT-$^{15}N_2$, 1.00 mg·kg$^{-1}$ of DiR) or lipo@DPT-$^{15}N_2$+$d_{10}$ (2.50 mg·kg$^{-1}$ of DPT-$^{15}N_2$+$d_{10}$, 1.00 mg·kg$^{-1}$ of DiR) for 24 h. The data are presented as mean ± SD (n = 5).

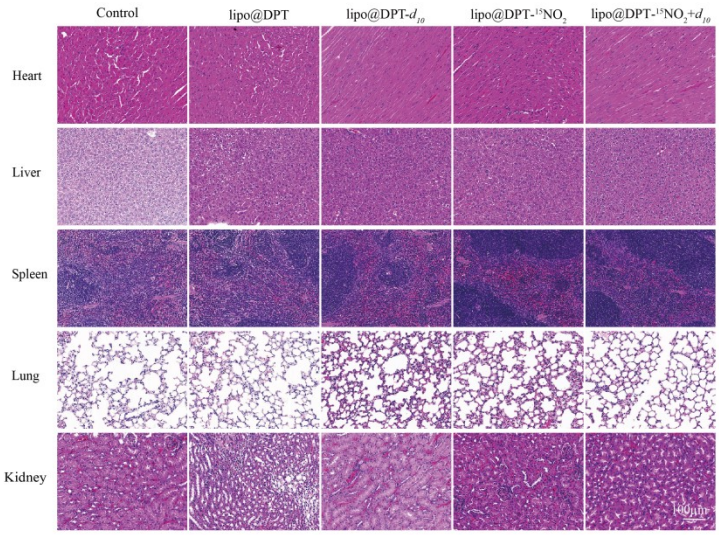


Figure S9 H&E histopathological analysis of major organ tissues. The data are presented as mean ± SD (n = 5).

Table S1 Encapsulation efficiency (EE) and drug loading rate (DL) of lipo@DPT, lipo@DPT-$d_{10}$, lipo@DPT-$^{15}N_2$, and lipo@DPT-$^{15}N_2$+$d_{10}$. The data are presented as mean ± SD (n = 6).

| | EE % | DL % |
|---|---|---|
| lipo@DPT | 94.54 ± 1.32 | 11.43 ± 2.13 |
| lipo@DPT-$d_{10}$ | 96.32 ± 2.51 | 10.33 ± 1.31 |
| lipo@DPT-$^{15}N_2$ | 95.64 ± 2.19 | 12.83 ± 1.67 |
| lipo@DPT-$^{15}N_2$+$d_{10}$ | 93.73 ± 2.23 | 12.45 ± 1.22 |

Table S2 Pharmacokinetic parameters of lipo@DPT, lipo@DPT-$d_{10}$, lipo@DPT-$^{15}N_2$, and lipo@DPT-$^{15}N_2$+$d_{10}$.

Parameters were calculated by PKSolver V2.0.

| PK parameters | DPT | DPT-$d_{10}$ | DPT-$^{15}N_2$ | DPT-$^{15}N_2$+$d_{10}$ |
|---|---|---|---|---|
| $T_{1/2}$ (h) | 2.02±0.29 | 4.00±0.45 | 2.20±0.31 | 4.20±0.65 |
| $AUC_{0\text{-}inf}$ (μg·h·mL-1) | 51.92±11.24 | 110±13.87 | 60±12.01 | 115±14.03 |
| $MRT_{0\text{-}inf}$ (h) | 2.915±0.36 | 5.77±0.76 | 3.18±0.43 | 6.06±0.83 |

## 2. Copies of identification spectra

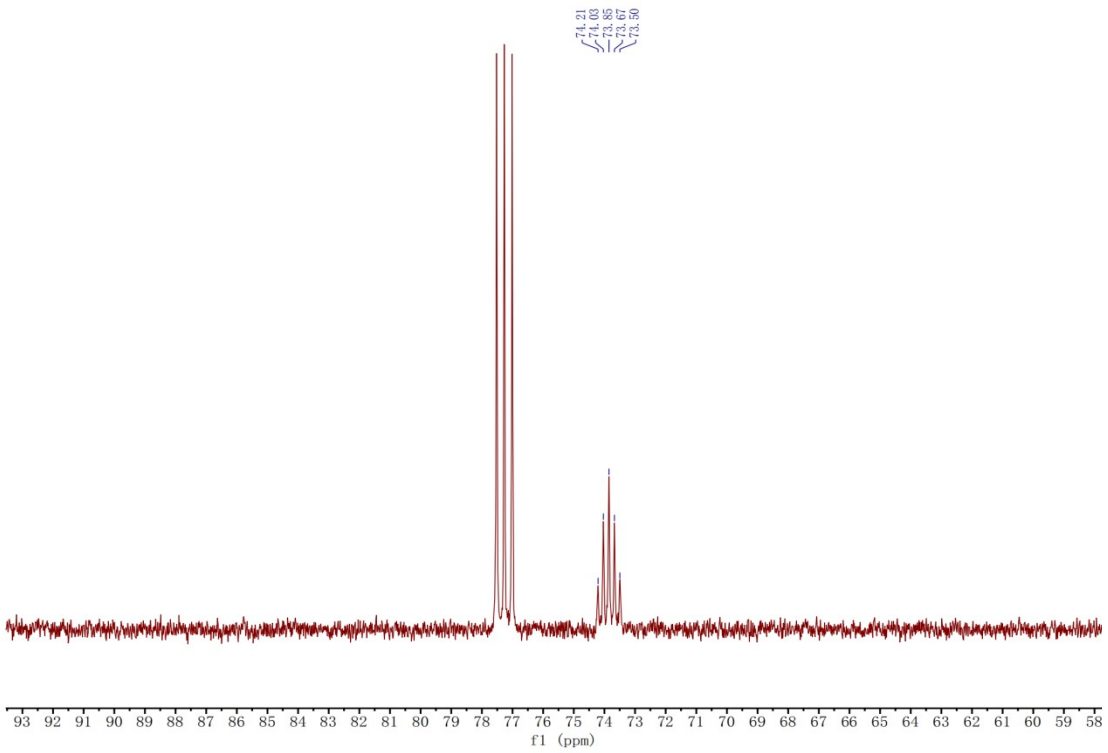


$^{13}$C-NMR spectrum of HA-$d_{12}$ (DMSO-$d_6$, 126 MHz)

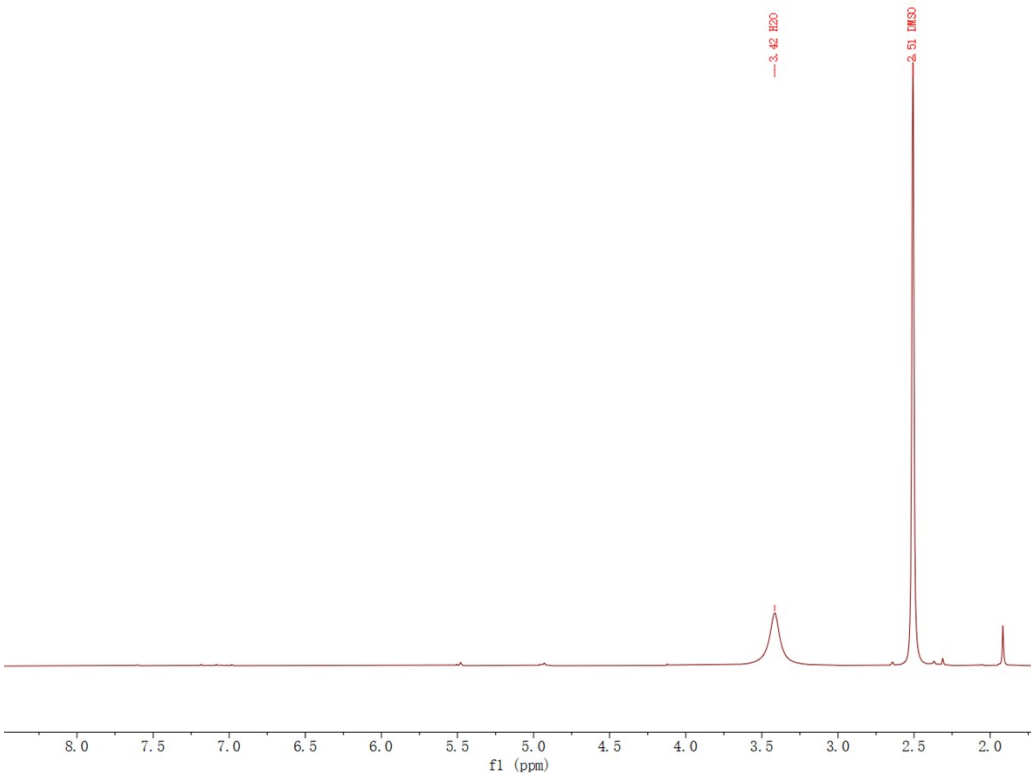


$^{1}$H-NMR spectrum of DPT-$d_{10}$ (DMSO-$d_6$, 500 MHz)

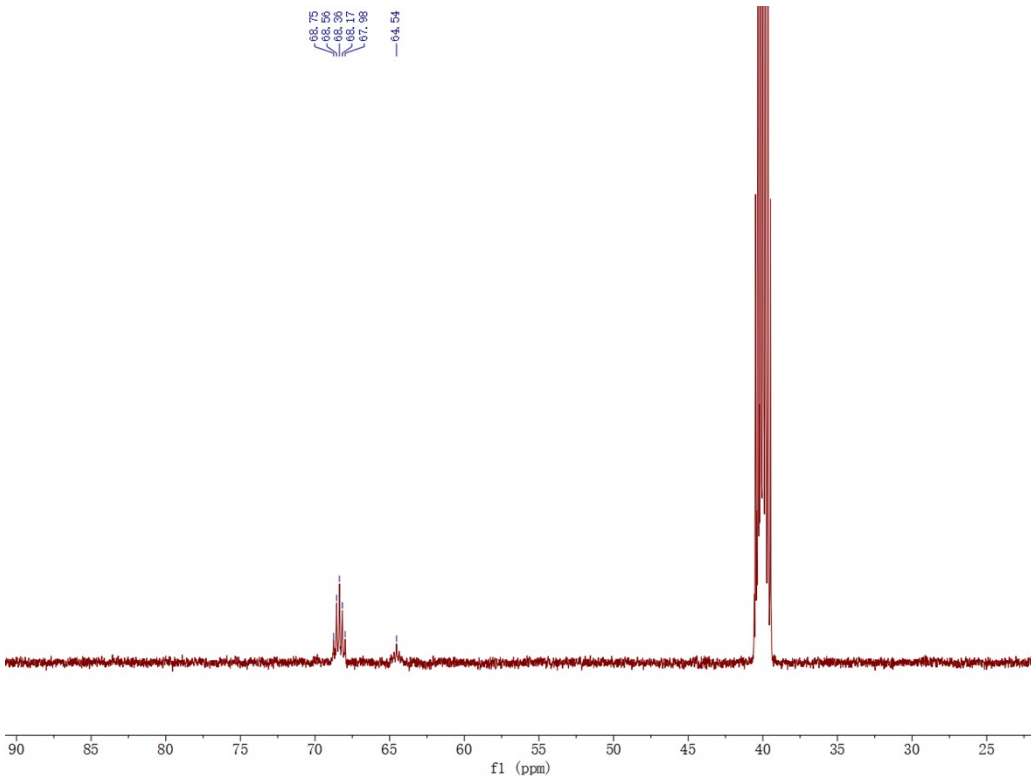


$^{13}$C-NMR spectrum of DPT-$d_{10}$ (DMSO-$d_6$, 126 MHz)

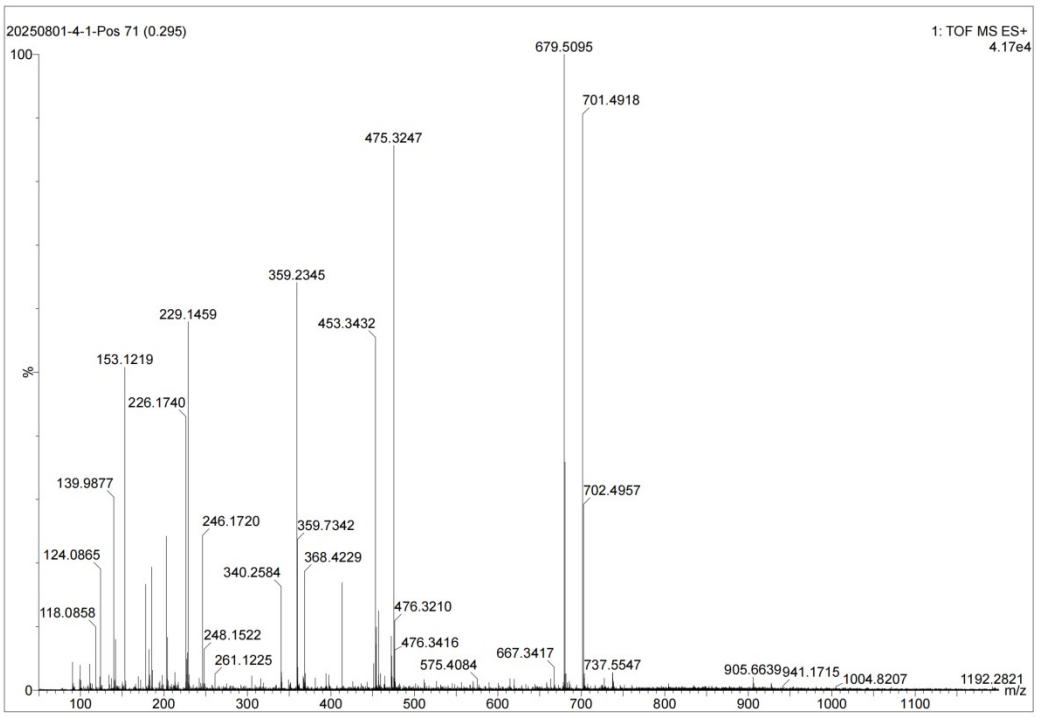


High-resolution mass spectrometry of DPT-$d_{10}$

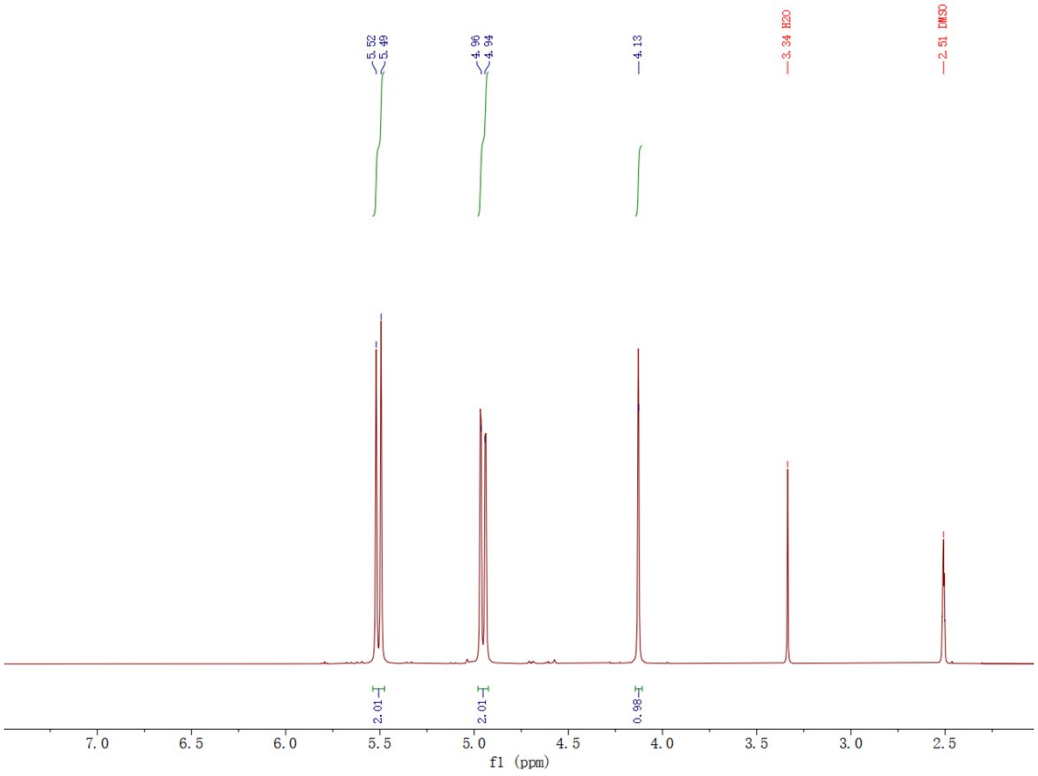


$^{1}$H-NMR spectrum of DPT-$^{15}N_2$ (DMSO-$d_6$, 500 MHz)

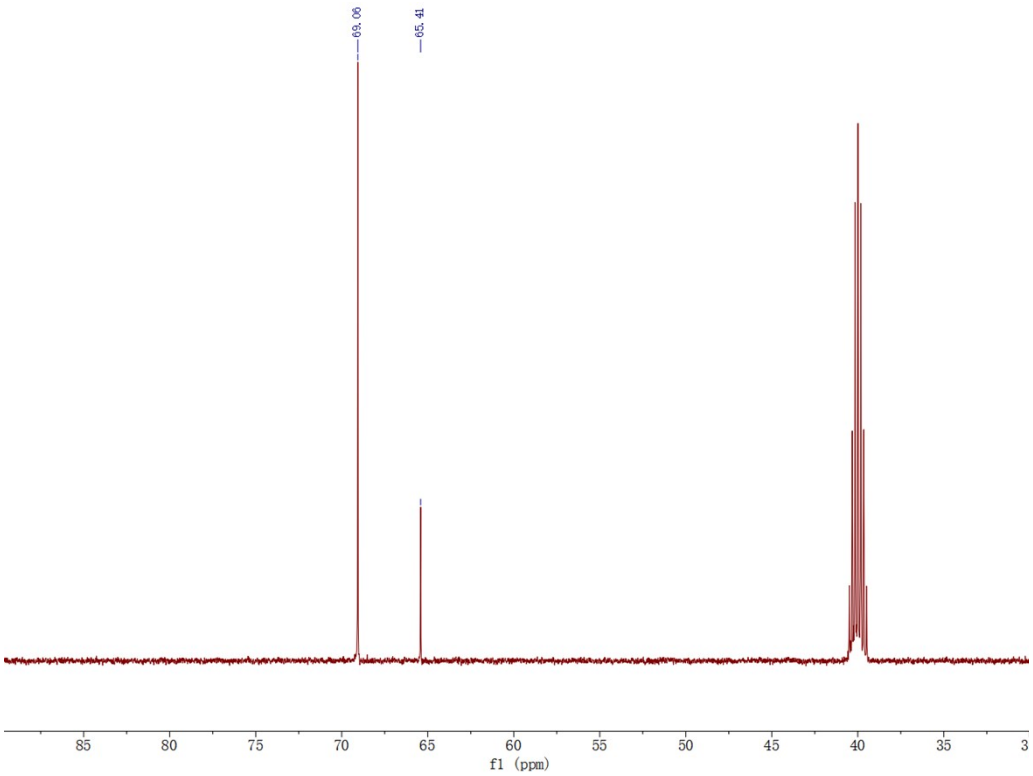


$^{13}$C-NMR spectrum of DPT-$^{15}N_2$ (DMSO-$d_6$, 126 MHz)

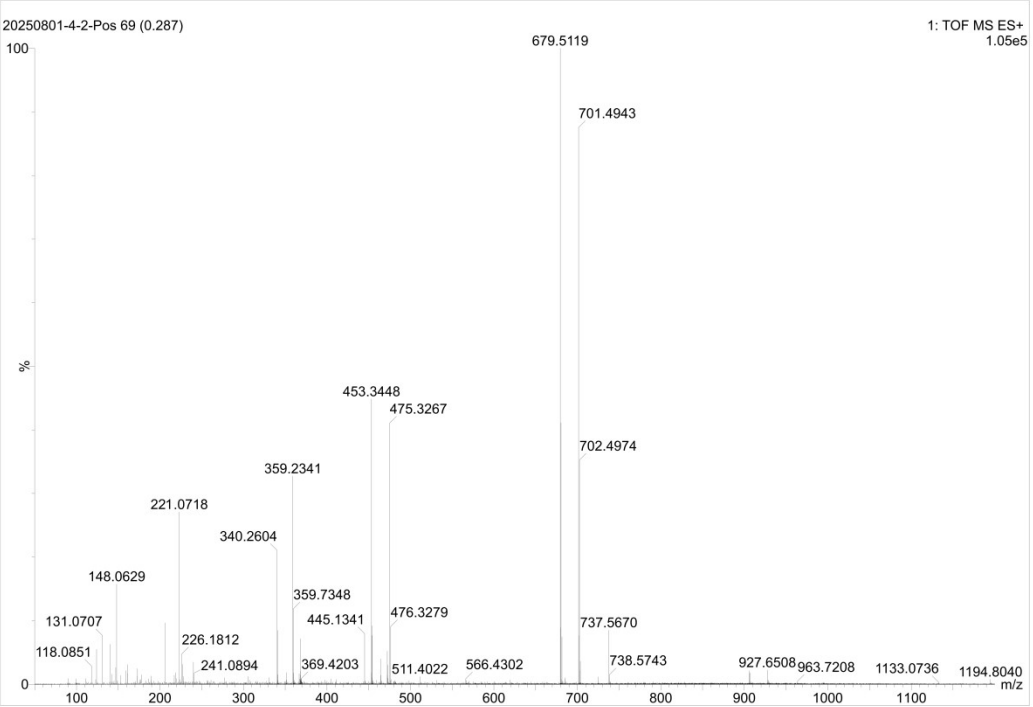


High-resolution mass spectrometry of DPT-$^{15}N_2$

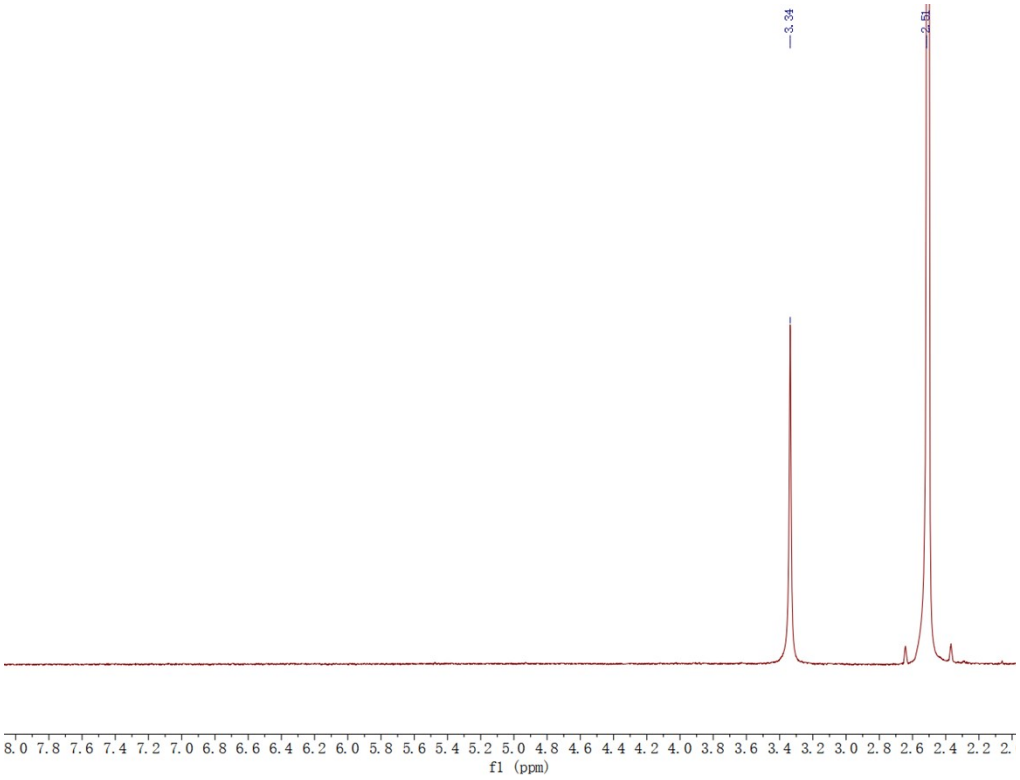


$^{1}$H-NMR spectrum of DPT-$^{15}N_2$+$d_{10}$ (DMSO-$d_6$, 500 MHz)

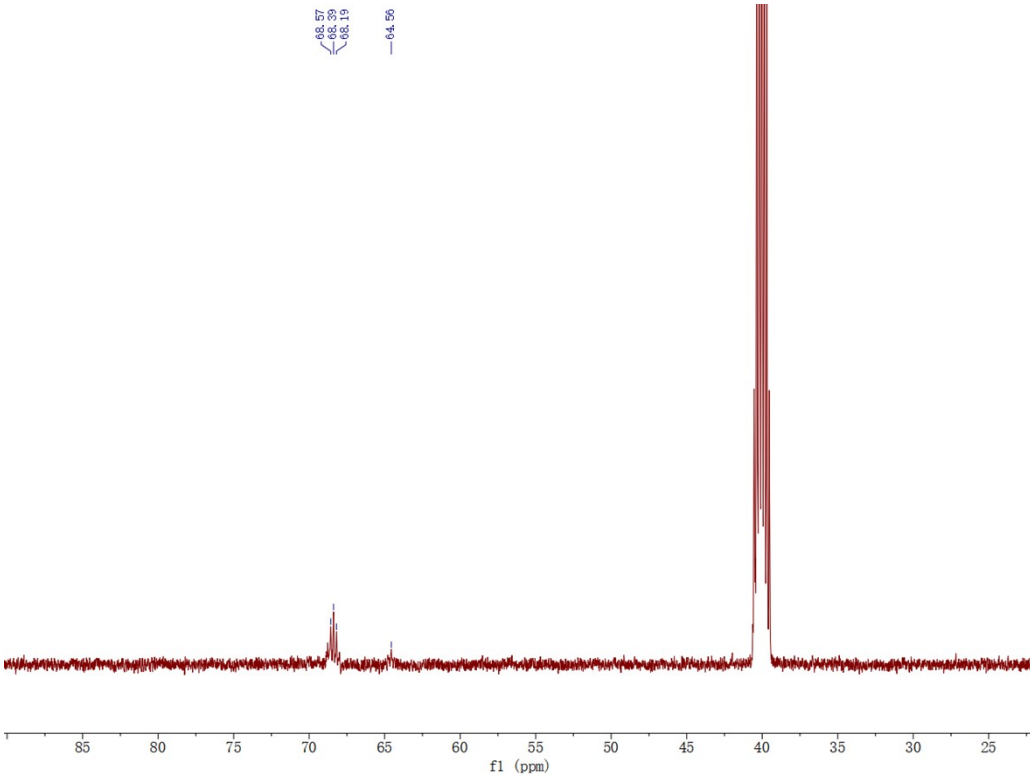


$^{13}$C-NMR spectrum of DPT-$^{15}N_2$+$d_{10}$ (DMSO-$d_6$, 126 MHz)

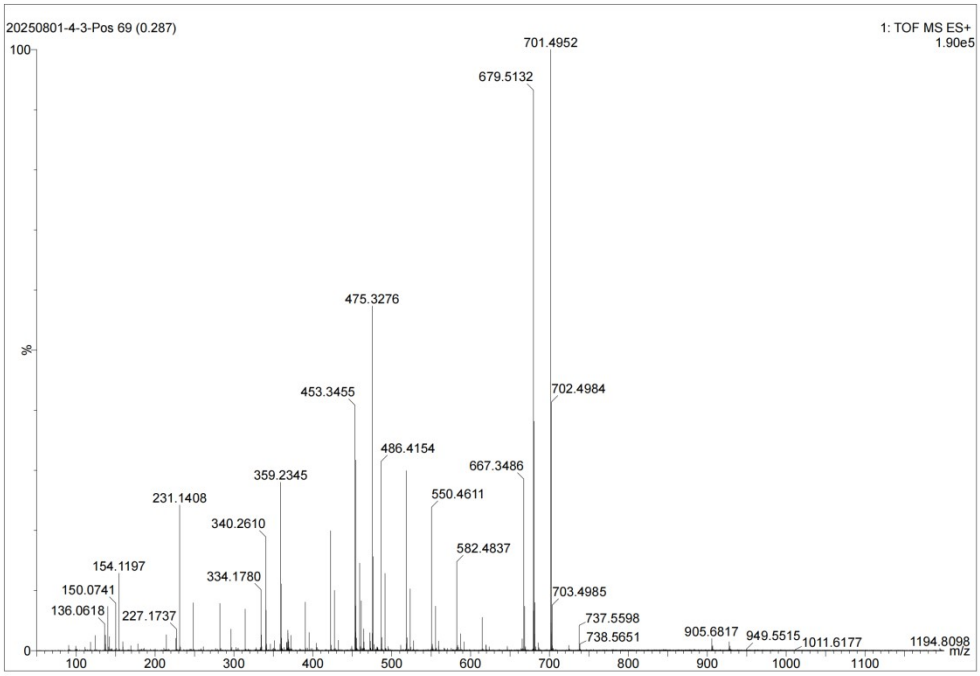


High-resolution mass spectrometry of DPT-$^{15}N_2$+$d_{10}$

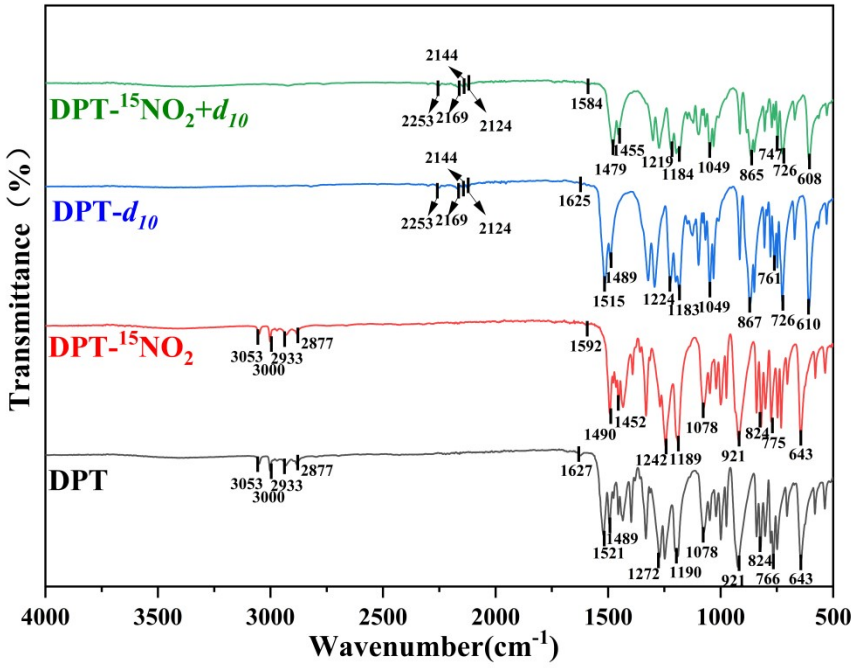


IR spectrum of DPT, DPT-$d_{10}$, DPT-$^{15}N_2$ and DPT-$^{15}N_2$+$d_{10}$